Use of LEED Intensity Oscillations in Monitoring Thin Film Growth†

D. K. Flynn, W. Wang, S.-L. Chang, M. C. Tringides, and P. A. Thiel*,‡

Departments of Chemistry and Physics and Ames Laboratory, Iowa State University, Ames, Iowa 50011

Received January 19, 1988. In Final Form: April 13, 1988

We show that a conventional LEED apparatus may be used to observe oscillations in diffracted intensity during growth of Pt on Pd(100). The oscillations are due to successive filling of Pt layers, exactly analogous to the oscillations often observed with RHEED during semiconductor growth. In spite of the rather small coherence length of the apparatus, the spot profiles consist of two well-separated components, which are due to short-range and long-range order.

Introduction

In recent years, relection high-energy electron diffraction (RHEED) has gained enormous popularity as a technique that can be used to measure the number of layers of material deposited during molecular beam epitaxy (MBE) of semiconductors. The technique rests upon the fact that the intensities of the reflected beams undergo periodic oscillations as a function of coverage during layer-by-layer growth, which are caused by morphological changes on the surface.[1-3] Intensity oscillations have been observed with RHEED during metal-on-metal growth as well.[4-6] Henzler and co-workers also report the use of a high-resolution LEED instrument to measure intensity oscillations during growth of Si on Si(111).[7] In this paper we show that a *conventional* low-energy electron diffraction (LEED) apparatus may be used in an exactly analogous manner to ascertain the growth characteristics of a metal-on-metal system. LEED optics are usually configured for normal beam incidence, and this fact (typically) makes LEED less convenient than RHEED as a tool to monitor deposition processes. Nonetheless, it is a technique which might fruitfully be applied in many laboratories using existing equipment. This is particularly significant, given the number of surface science groups currently initiating studies of metal-on-metal systems to understand bimetallic catalysts.

Experimental Section

The sample is mounted on a liquid-nitrogen cold finger[8] and is heated resistively by passing current through two 0.010-in.-diameter Ta wires spot-welded on one face or onto grooves cut in the edges of the sample. A W/5%Re vs W/26%Re thermocouple is spot-welded to the edge.

The Pd(100) sample is cleaned by prolonged ion bombardment at $T \geq 500$ K to remove sulfur and traces of phosphorus,[9-11] followed by repeated cycles of O_2 adsorption at room temperature and CO_g formation under vacuum at $T \geq 600$ K. The absence of CO evolution is taken to signal a carbon-free surface. At this point Auger electron spectroscopy (AES) usually indicates that the surface is also oxygen-free. Upon adsorption of CO, this surface also shows the normal sequence of CO-related LEED patterns, including $(\sqrt{2}\times 2\sqrt{2})R45°$ at $\theta_{CO} > 0.5$.[9-11]

The Pt evaporation source is based upon the design of De Cooman and Vook.[12] It consists of a Pt droplet melted into a gap between 0.020-in.-diameter tungsten rods, mounted on a commercial 2.75-in.-o.d. flange with high-current feedthroughs. To avoid contamination during evaporation, and also to reduce undesirable evaporation onto other vacuum chamber surfaces, the Pt filament is surrounded by a double-walled, liquid-nitrogen-cooled shroud mounted on a double-side flange. A 1-cm orifice in the shroud allows Pt vapor to escape toward the sample. When the apparatus is operating at sufficiently high temperatures, the evaporation filament is relatively adiabatic and the resultant Pt film is quite clean. Lower evaporation rates (lower temperatures) lead to gross carbon contamination. In a typical evaporation run the dc filament current is 47.5 A, and the pressure change in the chamber is about 6×10^{-10} Torr after 60 s. With the sample 1.5 cm away from the filament, the deposition rate at the sample is $(2-5) \times 10^{13}$ s^{-1} cm^{-2}. AES is used to check that the Pt distribution across the surface is uniform to within ±10%. There is no detectable evidence for Si, S, P, or C contamination in our Pt films or in the Pd substrate after cleaning. In all of the work described here, the films are deposited at a substrate temperature of 300-350 K and are not annealed. The results of annealing are discussed elsewhere.[13]

LEED spot profiles are measured with a computer-interfaced, silicon-intensified target video camera[14] and a standard set of Varian four-grid optics. The incident electron beam is normal to the surface within about 2°.

Results and Discussion

During adsorption of Pt at 300-350 K, LEED indicates that the Pt films grow isomorphically; i.e., the (1×1) periodicity of the Pd(100) substrate is always preserved. However, the full widths at half-maxima (fwhm) of the integral-order spot profiles vary strongly with incident beam voltage. The variation is such that at certain beam energies the spots for which $h + k = \pm 1, \pm 3, \ldots$ are very broad while the spots for which $h + k = 0, \pm 2, \ldots$ are very sharp. A photograph of the (1×1) pattern that illustrates this effect is shown in Figure 1. As the energy changes,

† Presented at the symposium on "Bimetallic Surface Chemistry and Catalysis", 194th National Meeting of the American Chemical Society, New Orleans, LA, Sept 1-3, 1987; B. E. Koel and C. T. Campbell, Chairmen.

‡ National Science Foundation Presidential Young Investigator (1985-1989), Alfred P. Sloan Foundation Fellow (1984-1986), and Camille and Henry Dreyfus Foundation Teacher-Scholar (1986-1990).

(1) Neave, J. H.; Joyce, B. A.; Dobson, P. J.; Norton, N. *Appl. Phys. A* **1983**, *31*, 1.
(2) Van Hove, J. M.; Lent, C. S.; Pukite, P. R.; Cohen, P. I. *J. Vac. Sci. Technol., B* **1983**, *1*, 741.
(3) Lewis, B. F.; Grunthaner, F. J.; Madhukar, A.; Lee, T. C.; Fernandez, R. *J. Vac. Sci. Technol., B* **1985**, *3*, 1317.
(4) Doyama, M.; Yamamoto, R.; Kaneko, T.; Imafuku, M.; Kokubu, C.; Izumiya, T.; Hanamure, T. *Vacuum* **1986**, *36*, 909.
(5) Bauer, E. In *RHEED and Reflection Electron Imaging of Surfaces*; Larsen, P. K., Ed.; Plenum: New York, in press.
(6) Purcell, S. T.; Heinrich, B.; Arrott, A. S. *Phys. Rev. B: Condens. Matter* **1987**, *35*, 6458.
(7) Horn, M.; Henzler, M. *J. Crystal Growth* **1987**, *81*, 428. Altsinger, R.; Busch, H.; Horn, M.; Henzler, M., to be published.
(8) Thiel, P. A.; Anderegg, J. W. *Rev. Sci. Instrum.* **1984**, *55*, 1669.
(9) Tracy, J. C.; Palmberg, P. W. *J. Chem. Phys.* **1969**, *51*, 4852.
(10) Behm, R. J.; Christmann, K.; Ertl, G.; Van Hove, M. A. *J. Chem. Phys.* **1980**, *73*, 2984.
(11) Ortega, A.; Hoffmann, F. M.; Bradshaw, A. M. *Surf. Sci.* **1982**, *119*, 79.
(12) DeCooman, B. C.; Vook, R. W. *J. Vac. Sci. Technol.* **1982**, *21*, 899.
(13) Beauvais, S. L.; Behm, R. J.; Chang, S.-L.; King, T. S.; Olson, C. G.; Rape, P. R.; Thiel, P. A. *Surf. Sci.* **1987**, *189/190*, 1069.
(14) Anderegg, J. W.; Thiel, P. A. *J. Vac. Sci. Technol. A* **1986**, *4*, 1367.

0743-7463/88/2404-1096$01.50/0

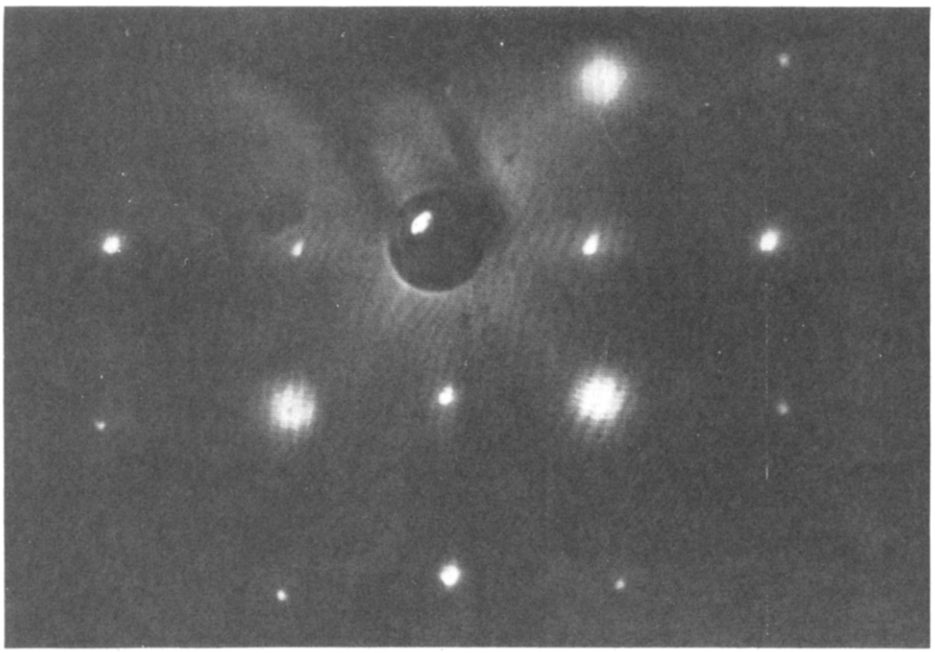

Figure 1. Photograph of a LEED pattern following evaporation of $^1/_3$ monolayer of Pt on Pd(100) at room temperature. Beam energy 150 eV, normal incidence.

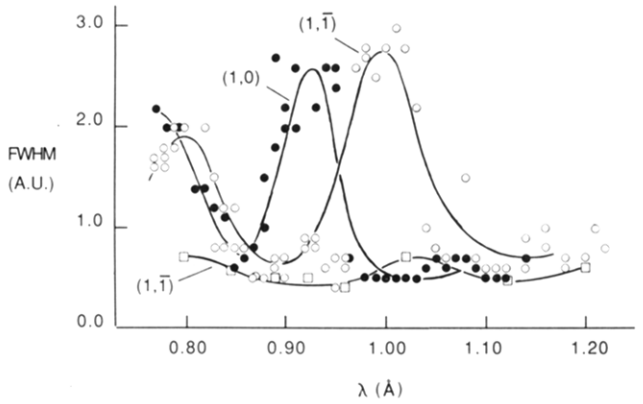

Figure 2. Variation in fwhm of spot profiles as a function of beam energy (electron wavelength) for a clean Pd(100) surface (squares) and after deposition of 2.5 monolayers of Pt at room temperature (circles). The fwhm are given in arbitrary units (A.U.).

the spots which are sharp broaden and vice-versa. These observations are qualitatively identical with those published by Wagner and Ross[15] in a study of electrochemical roughening of Pt(100) surfaces. These observations are shown quantitatively in Figure 2 for an initial Pt coverage of 2.5 monolayers.

These data can be interpreted within the framework developed by Henzler[16] and elaborated upon by Wagner and Ross.[15] Consider scattering from an island of atoms atop a square substrate, such as shown in Figure 3. We assume that the two-dimensional unit cell within each layer is identical, as shown. This is reasonable for the system under discussion. Scattering centers within the top layer are connected by a vector **g** to centers in the lower layer:

$$\mathbf{g} = x\mathbf{a} + y\mathbf{b} + \mathbf{c} \tag{1}$$

where **a** and **b** are the two-dimensional unit cell vectors of either plane and **c** connects the top and bottom planes. For an fcc lattice, $|\mathbf{a}| = |\mathbf{b}| = \sqrt{2}|\mathbf{c}|$, and the angle between each pair of vectors is $\pi/2$.

(15) Wagner, F. T.; Ross, P. N., Jr. *Surf. Sci.* **1985**, *160*, 305.
(16) Henzler, M. *Surf. Sci.* **1970**, *22*, 12.

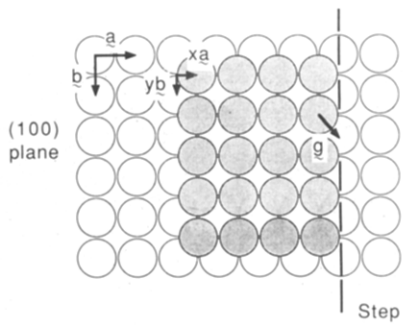

Figure 3. Schematic depiction of an fcc (100) surface (open circles) with an island of atoms in a top layer (shaded circles). The real-space vectors are used in the text.

The phase difference between adjacent terraces is given by

$$\mathbf{g}\cdot\Delta\mathbf{k} = 2n\pi \tag{2}$$

where $\Delta\mathbf{k}$ is the momentum-transfer wave vector. The parameter n is an integer for constructive interference or half-integer for destructive interference. Introducing the reciprocal-space vectors **a***, **b***, and **c*** and setting

$$\Delta\mathbf{k} = h\mathbf{a}^* + k\mathbf{b}^* + l\mathbf{c}^* \tag{3}$$

eq 2 becomes

$$(x\mathbf{a} + y\mathbf{b} + \mathbf{c})(h\mathbf{a}^* + k\mathbf{b}^* + l\mathbf{c}^*) = 2n\pi \tag{4}$$

or

$$xh + yk + l = n \tag{5}$$

Here h and k must be integers, and l is determined by the component of $\Delta\mathbf{k}$ normal to the surface. In terms of experimental parameters, l is determined by the electron wavelength (beam energy) and by the diffraction spot indices, h and k. Henzler[16] has shown that, for normal incidence

$$l = (|\mathbf{c}|/2\pi)(|\mathbf{k}_0| + [|\mathbf{k}_0|^2 - |(h\mathbf{a}^* + k\mathbf{b}^*)|^2]^{1/2}) \tag{6}$$

When $(h\mathbf{a}^* + k\mathbf{b}^*)^2$ is small compared with $\mathbf{k}_0^2$, then l is determined only by the beam energy, V_e, and eq 5 reduces to

$$V_e = (150.4/4|\mathbf{c}|^2)(n - xh - yk)^2 \tag{7}$$

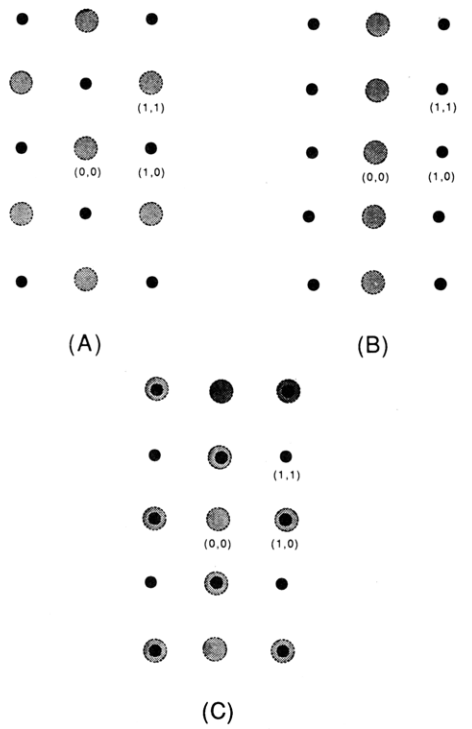

Figure 4. Schematic depiction of possible patterns of spot broadening induced by steps, as discussed in the text. (A) $x = y = {}^1/_2$; fourfold hollow sites occupied. (B) $x = {}^1/_2$, $y = 0$; one domain of twofold bridge sites occupied. (C) $x = {}^1/_2$,0 and $y = 0,{}^1/_2$; two domains of twofold bridge sites, patterns overlaid.

It is easy to show that the patterns of in-phase and out-of-phase scattering shown in Figure 4 will result from the indicated choices of x and y, under these conditions. For instance, choose $x = y = {}^1/_2$ in eq 5. The spot described by $h = 0$, $k = 1$ is in-phase when $n = {}^1/_2 + l$ is an integer, whereas coherent scattering at $h = 1$, $k = 1$ requires that $n = 1 + l$ is an integer. In other words, when the (0,1) spot is in-phase, the (1,1) spot is exactly out-of-phase (n differs by ${}^1/_2$) for these choices of x and y. This provides a qualitative explanation for our results, which are most consistent with the choice $x = y = {}^1/_2$. These values for x and y require that the Pt atoms occupy fourfold hollow sites, which is physically reasonable for an fcc metal growing atop another fcc metal with an almost identical lattice constant.

However, in LEED it is not usually valid to assume that

$$(h\mathbf{a}^* + k\mathbf{b}^*)^2 \ll \mathbf{k}_0{}^2 \tag{8}$$

in eq 6. For the Pt on Pd system, with $x = y = {}^1/_2$, this means that the (0,1) spot is not in-phase at *exactly* the same energy where the (1,1) spot is out-of-phase, for instance. Rather, there is a constant difference of about 10 eV between the energies where eq 5 predicts that these two conditions are met, in the range from 50 to 300 eV. The trend and symmetry shown in Figure 4a are preserved, however.

By concentrating on a single beam and measuring the angular profile half-width as a function of energy, we can extract information about the surface step height. When n is an integer, the half-width is expected to be a minimum since the scattered electrons interfere constructively;[17] when n is a half-integer, maximum destructive interference occurs between terraces and the profile is broader. Thus, the profile half-width oscillates with energy as observed in Figure 2. From the period of oscillations the step height, c, can be extracted. The resultant value is 2.0 ± 0.1 Å, identical within experimental uncertainty with the bulk value (1.96 Å for Pt). In the same figure at the bottom (using square symbols), we show similar measurements for clean Pd(100), but only very weak oscillations are seen. This probably means that the instrument coherence length, L [i.e., the maximal resolvable distance where coherent scattering occurs[18]], is smaller than the average terrace site, M. From the observed energy-independent half-width we estimate $L \approx 100$ Å and from the misorientation of the crystal (0.5°) $M \approx 220$ Å.

We can interpret our results in terms of a classic two-level system[19,20] resulting from overlayer deposition. The diffracted intensity exhibits oscillations, corresponding to a maximum when full layers are complete and a minimum at half-monolayers. More precisely, the angular profile of a two-level system consists of a sharp instrument-limited part superimposed on a diffuse background.[19,20] The sharp contribution results from coherent scattering of all the atoms present (both substrate and overlayer) and the broad part from incoherent scattering of the overlayer islands. As can be seen from Figure 5, the measured profiles indeed display such form, especially at coverages intermediate between completion of full layers. These measurements are performed on the (1,$\bar{1}$) beam at the out-of-phase condition, where sensitivity to the surface morphology is maximum. A good measure of the top-layer occupation (and therefore the Pt coverage) is the peak intensity, I_p, of the sharp portion. This quantity is represented schematically in the inset to Figure 6. It can be shown[19,20] that

$$I_p \propto (2\theta_{Pt} - 1)^2 \tag{9}$$

where θ_{Pt} is the Pt coverage. It is clear from this expression that I_p is a maximum when $\theta_{Pt} = 0$ or 1 and a minimum when $\theta_{Pt} = 0.5$. This creates intensity oscillations with constant amplitude as more layers are deposited if perfect layer-by-layer filling (Frank van der Merwe growth) takes place. Oscillations are apparent in the data of Figure 6, supporting our previous report of layer-by-layer growth in this system.[13] Actually, as can be seen from Figure 6, the oscillation amplitude is not constant, but rather decays with time (coverage), suggesting that more and more levels are partially occupied at the coverages corresponding intensity maxima. The atoms on these levels scatter incoherently, reducing the maximum peak intensity. The points where the intensity maxima occur suggest $\theta_{Pt} \sim 1$, 2, 3 etc., and they correspond to Pt:Pd Auger ratios[13] of 0.3, 0.8, and 1.2, respectively. This coverage calibration (in terms of the Auger ratios) is in excellent agreement with our previous coverage determination,[13] which was based only on Auger and ultraviolet photoemission spectroscopies. Furthermore, the nearly linear variation of film coverage with evaporation time indicates that the Pt sticking coefficient is constant under these evaporation conditions, i.e., it is independent of changes in surface morphology and composition as the film grows. A constant sticking coefficient is usually assumed implicitly (and without justification) in studies of metal film growth.

It is interesting to notice that although the instrument has low resolving power we are still able to separate the coherent scattering from the diffuse part. This is because only small Pt islands form during film growth, as can be

(17) Lagally, M. G.; Savage, D.; Tringides, M. C. In *RHEED and Reflection Electron Imaging of Surfaces*, Larsen, P. K., Ed.; Plenum: New York, in press.

(18) Lu, T.-M.; Lagally, M. G. *Surf. Sci.* **1980**, *99*, 695.
(19) Lent, C. S.; Cohen, P. I. *Surf. Sci.* **1984**, *139*, 121.
(20) Pimbley, J. M.; Lu, T.-M. *J. Appl. Phys.* **1985**, *57*, 1121.

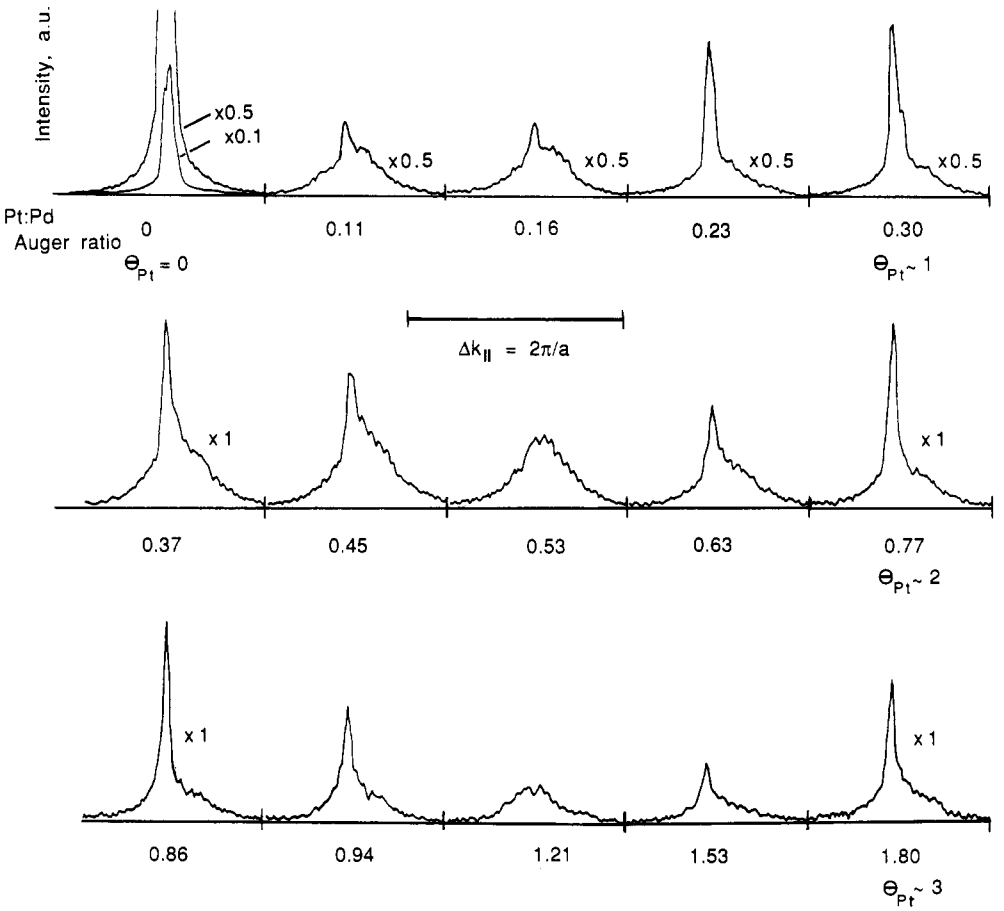

Figure 5. Profiles of the $(1,\bar{1})$ spot after successive Pt evaporations. Each profile is labeled with the Auger intensity ratio, denoted Pt:Pd.[13] Profile intensities are given in arbitrary units. Coverages are also given for selected profiles. The Pt coverages are in excellent agreement with other work,[13] in which Auger and ultraviolet photoemission spectroscopies are used to infer coverages but not LEED.

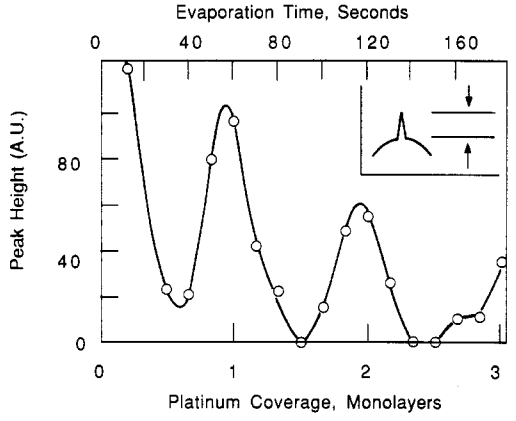

Figure 6. Variation of LEED spot intensity (given in arbitrary units) as a function of evaporation time and Pt coverage. The inset shows schematically how the peak height, I_p, is obtained from each profile.

seen from the large half-width of the diffuse part (corresponding to an island diameter of only 10 Å), which stays invariant with coverage. Because this length is much smaller than the coherence of the instrument, the diffuse contribution is well separated.

One interesting aspect of the data is the presence of Lorentzian-like wings in the initial profile and in the profiles measured after completion of each Pt layer. This is not unreasonable after the completion of 1, 2, 3 ... layers because, as stated previously, there is an increasing tendency for some atoms to occupy higher levels, and this causes the oscillation amplitude to decrease by transferring diffracted intensity to the wings. However, wings are also present in the very first profile, which results from a clean surface. This profile should be instrumentally limited and therefore should be Gaussian, since the terrace length is larger than the coherence length. Perhaps some part of its Lorentzian-like shape is due to the presence of a small percentage of point defects on the clean Pd surface, but we do not believe this can account for all of its deviation from a Gaussian profile.

We conclude by considering some practical aspects of LEED, as it is typically configured, in terms of the convenience and data acquisition capabilities necessary for a study such as we describe here.

First, in order to obtain a set of data such as shown in Figure 5, our chamber configuration requires that we deposit a small amount of Pt film, turn the sample 180° to face the Auger spectrometer, measure the resultant film coverage, and then turn the sample again by 90° to face the LEED optics. This entire process, plus the measurement of eight spot profiles using the video camera and computer, takes about 5–6 min. Thus, where RHEED can be used to measure overlayer characteristics continuously during deposition, the analogous LEED measurement (at least in our apparatus) is a sequential one, and deposition cannot take place continuously. This is one of the disadvantages of LEED in comparison to RHEED. Continuous measurement during deposition is possible with RHEED because the glancing incident and exit angles allow the electron gun and detector to be positioned well out of way of the evaporation source, which can then face the sample directly. In principle, LEED could also be configured to permit constant spot profile measurement during continuous deposition, but most chambers currently in use would

not readily lend themselves to such an adaptation, because the LEED optics are arranged for normal incidence. A sequential experiment, such as we describe here, would often be possible, however.

Second, it is necessary to use some type of data acquisition system that is reasonably fast, i.e., a system that can gather the necessary spot profiles within a minute or two. This is because the sample is prone to contamination in the time between depositions. The data acquisition process should be relatively fast so as not to lengthen the experiment significantly. The video system which we use[14] is convenient, although many other techniques (e.g., photography or resistive anode networks) could certainly be used as well.

In summary, we observe diffracted intensity oscillations in the growth of Pt on Pd(100) with a conventional LEED diffractometer. All our observations are similar to the oscillations usually observed in semiconductor MBE growth. This is a preliminary report, and more systematic results will be presented after the completion of experiments still in progress. More quantitative information will be extracted from the angular profile line shapes by taking into account the instrumental resolution.

Acknowledgment. This work is supported by a Presidential Young Investigator Award of the National Science Foundation, Grant No. CHE-8451317. In addition, some equipment and all facilities are provided by the Ames Laboratory, which is operated for the U.S. Department of Energy by Iowa State University under Contract No. W-7405-ENG-82.

Registry No. Pt, 7440-06-4; Pd, 7440-05-3.

Reactions of 2,2-Dimethylbutane on $Pt/Re/Al_2O_3$ Catalysts. Effect of Sulfur and Chlorine on the Selectivity†

A. J. den Hartog, P. J. M. Rek, M. J. P. Botman, C. de Vreugd, and V. Ponec*

Gorlaeus Laboratories, Leiden University, P.O. Box 9502, 2300 RA Leiden, The Netherlands

Received December 29, 1987. In Final Form: April 20, 1988

Reactions of 2,2-dimethylbutane (neohexane) have been studied with two series of $Pt/Re/Al_2O_3$ catalysts: one prepared chlorine-free, the other prepared from chloride(s) as precursor(s). The catalysts have been studied in the reduced, unsulfided state and after presulfidization by thiophene. It appears that both metallic (catalyst) components form clusters (alloys): their catalytic behavior is "nonadditive". After sulfidization of the catalysts, the relative role of acid-catalyzed reactions increases.

Introduction

The supported Pt/Re alloys (or bimetallic clusters) have attracted a lot of attention since the first report on the superior behavior of these materials in 1968.[1,2] The first generation Pt catalyst ("mono metal") has been replaced in the naptha reforming shortly afterwards by the Pt/Re catalysts that are today the most frequently used catalysts in this branch of petrochemistry. Fundamental studies devoted to the Pt/Re alloys have been already performed as well, as can be illustrated by a small selection of papers.[1,3-7]

The superior behavior of the Pt/Re catalysts as compared with the Pt catalysts has given rise to the formulation of several theories to explain this fact. For the benefit of the reader, various theories are summarized below into the following groups.

(1) Re influences the deposition of carbon on the acidic support. The function of Re, either in the oxidic or metallic form, is to promote the fission or other ways of removal of the coke precursors, thus preventing the self-poisoning of the catalysts.[8-10]

(2) Re modifies the availability and reactivity of hydrogen on the catalyst surface by influencing such phenomena like the "spillover" of hydrogen.[11,12]

(3) Re functions as an anchor preventing the sintering of the Pt particles and possibly influences the properties of the Pt catalyst as well.[13-15]

(4) Re forms an irreversible sulfide during sulfidization as the bond strength of Re-S is larger than that of Pt-S.

* Author to whom all correspondence should be sent.

† Presented at the symposium on "Bimetallic Surface Chemistry and Catalysis", 194th National Meeting of the American Chemical Society, New Orleans, LA, Sept 1-3, 1987; B. E. Koel and C. T. Campbell, Chairmen.

(1) Charcosset, H. *Rev. Inst. Fr. Pet.* **1979**, *34*, 238. Charcosset, H. *Int. Chem. Eng.* **1983**, *23*, 411.
(2) Kluksdahl, H. E. *U.S. Patent* 3 415 737, 1968. Jacobson, R. L.; Kluksdahl, H. E.; McCoy, C. S.; Davis, R. W. In *Proc.-Am. Pet. Inst., Div. Refin.* **1969**, 504.
(3) Haining, I. H. B.; Kemball, C.; Whan, D. A. *J. Chem. Res. Symp.* **1978**, 364; **1977**, 170.
(4) Betizau, C.; Leclercq, G.; Maurel, R.; Bolivar, C.; Charcosset, H.; Frety, R.; Tournayan, L. *J. Catal.* **1976**, *45*, 179. Bolivar, C.; Charcosset, H.; Frety, R.; Primet, M.; Tournayan, L.; Betizau, C.; Leclercq, G.; Maurel, H. *J. Catal.* **1975**, *39*, 249; **1976**, *45*, 163. Charcosset, H.; Frety, R.; Leclercq, G.; Mendes, E.; Primet, M.; Tournayan, L. *J. Catal.* **1979**, *56*, 468.
(5) Biloen, P.; Helle, J. N.; Verbeek, H.; Dautzenberg, F. M.; Sachtler, W. M. H. *J. Catal.* **1980**, *63*, 112. Sachtler, W. M. H.; Biloen, P. *Prepr.*-Am. Chem. Soc., Div. Pet. Chem. **1983**, 482.
(6) Shum, V. K.; Butt, J. B.; Sachtler, W. M. H. *J. Catal.* **1985**, *96*, 371; **1986**, *99*, 126.
(7) Coughlin, R. W.; Hasan, A.; Kawakami, K. *J. Catal.* **1984**, *88*, 150; **1984**, *88*, 163.
(8) Ludlum, L. H.; Eischens, R. P. *Prepr.*-Am. Chem. Soc. Div. Pet. Chem. **1976**, 375.
(9) Burch, R.; Mitchell, A. *J. Appl. Catal.* **1983**, *6*, 121.
(10) Bertolacini, R. J.; Pellet, R. J. In *Catalyst Deactivation*; Delmon, B., Froment, G. F., Eds.; Elsevier: Amsterdam, 1980; p 73.
(11) Margitfalvi, J.; Göbölös, S.; Kwaysser, E.; Hegedus, M.; Nagy, F.; Koltai, L. *React. Kin. Catal. Lett.* **1984**, *24*, 315.
(12) Traffano, E. M.; Parera, J. M. *Appl. Catal.* **1986**, *28*, 193.
(13) Yermakov, Yu, I.; Kuznetsov, B. N. *J. Mol. Catal.* **1980**, *9*, 13.
(14) Engels, S.; Wilde, M.; Tran Kim Thanh *Z. Chem.* **1977**, *17*, 10.
(15) Graham, A. G.; Wanke, S. E. *J. Catal.* **1981**, *68*, 1.

0743-7463/88/2404-1100$01.50/0